Three-dimensional Fermi-surface nesting in $1T$-VSe$_2$ studied by angle-resolved photoemission spectroscopy

Takafumi Sato, Kensei Terashima, Seigo Souma, Hiroaki Matsui, Takashi Takahashi,

Hongbo Yang[1], Shancai Wang[1], Hong Ding[1], Nobuhiro Maeda[2], and Koya Hayashi[2]

Department of Physics, Tohoku University, Sendai 980-8578

[1]*Department of Physics, Boston College, Chestnut Hill, MA 02467, USA*

[2]*Okayama University of Science, 1-1 Ridai-cho, Okayama 700-0005*

We have performed high-resolution angle-resolved photoemission spectroscopy (ARPES) with synchrotron radiation on layered transition-metal dichalcogenide $1T$-VSe$_2$ to study the mechanism of the three-dimensional charge-density-wave (CDW) transition. We found that the Fermi surface around the M(L) and K(H) points shows considerable wiggling along the wave vector normal to the layer (k_z) despite the apparently two-dimensional crystal structure. ARPES spectra below the CDW transition temperature show a signature of pseudogap opening at a specific k_z-region on the Fermi surface, demonstrating that the CDW transition of $1T$-VSe$_2$ is driven by three-dimensional Fermi-surface nesting.

KEYWORDS: photoemission, $1T$-VSe$_2$, charge-density wave, Fermi surface

1. Introduction

Layered transition-metal dichalcogenide (TMDC) $1T$-VSe$_2$ shows charge-density-wave (CDW) transition at $T_c = 110$ K, accompanied by distinct anomalies in the transport,[1] thermodynamic,[1–3] magnetic,[1] and spectroscopic[4–14] properties. X-ray and electron-diffraction experiments[15, 16] provided an evidence for a periodic lattice distortion (PLD) below T_c, by observing the 4×4 superlattice spot within the layer. It has also been reported that the PLD wave vector has a substantially large component perpendicular to the layer comparable to a 1/3 of the height of the Brillouin zone (BZ),[15, 16] suggesting a three-dimensional nature of the CDW formation in $1T$-VSe$_2$. In order to clarify the mechanism of CDW transition in $1T$-VSe$_2$, high-resolution angle-resolved photoemission spectroscopy (ARPES) with fixed photon energy has been performed, reporting a partial Fermi-surface (FS) nesting on the electron-like FS centered at the M(L) point.[17] In addition, the previous ARPES observed substantial suppression of the spectral weight below T_c around the nested portion of the FS, suggesting that the CDW transition in $1T$-VSe$_2$ is caused by the three-dimensional FS nesting. However, there is no direct evidence for whether or not the FS nesting is actually three-dimensional, since the previous ARPES experiment with fixed photon energy[17] lacks the information on the electronic structure normal to the layer because the momentum normal to the layer was

not tunable in the experiment.

In this paper, we report high-resolution ARPES on $1T$-VSe$_2$ with tunable-energy photons from synchrotron radiation. We have succeeded in directly observing the band dispersion perpendicular to the layer and found that the electronlike FS shows a considerable wiggling in the momentum region midway between M(K) and L(H) points in the BZ, producing a fairly straight portion of FS in a specific k_z-region. We found that a pseudogap opens at this flat FS portion, while no signature for pseudogap opening was observed in other region. These experimental results provide a definite evidence for the three-dimensional FS nesting in $1T$-VSe$_2$. We have compared the present ARPES results with the band structure calculation as well as the Hall coefficient and magnetic susceptibility measurements to discuss the shape of FS and the number of carriers which participate in the CDW transition.

2.   Experiments

Single crystals of $1T$-VSe$_2$ were grown by the chemical vapor transport method. Starting materials were 99.5 % vanadium powder and selenium shot. Crystals were grown in an evacuated sealed quart tube by excess-selenium vapor transport at 700°C for 7 days after being preheated at 850°C for 3 days. The obtained crystals are platelet and as large as 5×5×0.1 mm^3. The thermogravimetric analysis shows that the crystals are stoichiometric within a 1 % experimental accuracy.[18]

ARPES measurements were performed using a GAMMADATA-SCIENTA SES-200 spectrometer at undulator 4m-NIM (normal incidence monochromator) and undulator PGM (plane grating monochromator) beam lines in Synchrotron Radiation Center, Wisconsin. The energy and angular resolutions were set at 10-25 meV and 0.3°, respectively. Clean surface for ARPES measurements was obtained by *in-situ* cleaving of crystal in an ultrahigh vacuum better than 7x10^{-11} Torr. The Fermi level (E_F) of the sample was referenced to that of a gold film evaporated onto the sample substrate.

3.   Results and discussion

Figure 1(a) shows normal-emission ARPES spectra of $1T$-VSe$_2$ measured at 40 K with various photon energies from $h\nu = 17$ to 36 eV. We at first notice a non-dispersive sharp peak in the vicinity of E_F in all spectra. We also find another weak non-dispersive structure at about 2 eV binding energy. The non-dispersive character of these peaks indicates that they are assigned to Se $4p$ σ ($4p_{x,y}$) orbitals.[11, 12, 19, 20] In addition to these non-dispersive bands, there are several dispersive bands as seen in Fig. 1(a). The most prominent dispersive band has the bottom of dispersion around 3.5 eV binding energy at $h\nu = 23.5$ eV and disperses toward E_F with increasing/decreasing $h\nu$. In the higher-binding energy region, we find another dispersive band, which has the top of dispersion around 4.5 eV binding energy at $h\nu = 23.5$ eV and disperses toward higher binding energy on increasing $h\nu$. This band shows a bottom

of dispersion at about 6 eV at $h\nu = 33$ eV and turns to disperse back toward E_F on further increasing $h\nu$. These two bands are assigned to Se $4p$ π ($4p_z$) orbitals[11, 12, 19, 20] because of the strongly dispersive nature perpendicular to the layer (k_z direction). The observed symmetric behavior of dispersion with respect to the spectra at $h\nu = 23.5$ and 33 eV indicates that these photon energies correspond to high-symmetry points along the ΓA direction in BZ, namely Γ or A point.

To see more clearly the dispersive feature of bands in the ARPES spectra, we have mapped out the experimental band structure as a function of k_z as shown in Fig. 1(b). The experimental band structure has been obtained by taking the second derivative of ARPES spectra and plotting the intensity with gray scale as a function of k_z and binding energy. Bright areas correspond to bands. In the process of band mapping, we have determined the inner potential V_0 to be 6.6 eV, with which the experimental band dispersion shows a good matching with the periodicity of BZ of 1T-VSe$_2$. This value is in accordance with the valence-band width of about 6 eV, and is also consistent with previous ARPES report.[12] In Fig. 1(b), we show the band calculation for 1T-VSe$_2$ using the linear augmented plane wave (LAPW) method[11] for comparison. As seen in Fig. 1(b), most of experimentally obtained bands show a fairly good correspondence to the calculated bands. The observed significantly large bandwidth (2 eV) of p_z and p_z* bands indicates that 1T-VSe$_2$ has a substantially three-dimensional electronic structure despite the apparent layered crystal structure. We also find finite differences between present experiment and the calculation. Dispersive feature around 5-6 eV at $k_z = 2.3$ - 2.4 $\mathring{A}^{-1}$ would be produced by an inelastic secondary-photoelectron emission,[12] while the spectral intensity around 1 eV at $k_z = 2.8$ $\mathring{A}^{-1}$ and that around 2-3 eV at $k_z = 3.2$ $\mathring{A}^{-1}$ may be attributed to the final-state band-structure effect and/or the self-energy effect, as has been discussed previously.[12]

Next we show ARPES results near the M(L) point, since the FS in this momentum region is expected to participate in the CDW formation.[17] Figures 2(a) and (b) show the plane in the reciprocal space where ARPES measurements were actually done by changing the photon energy. It is noted that the plane is rotated by 15° with respect to the MKLH plane. We define three axes (k_x, k_y, k_z) in this plane as shown in Fig. 2(b). The reason why we chose this plane is that we can track the E_F-crossing points of V $3d$ bands in all k_z area of the first BZ, since the FS is located always midway between the M(L) and K(H) points. Figures 2 (c)-(e) show ARPES-intensity plots for three different photon energies, where we clearly find a single band which shows a distinct energy dispersion of more than 0.4 eV and an abrupt intensity drop at E_F due to the E_F-crossing. We have determined the E_F-crossing points (denoted by arrows in Figs. 2 (c)-(e)) by fitting the momentum distribution curves, and found that the k_z of E_F-crossing points (k_{Fy}) is not constant but varies systematically as a function of $h\nu$. For example, k_{Fy} for $h\nu = 35$ eV is 0.12 $\mathring{A}^{-1}$ while that for $h\nu = 27$ eV is 0.03 $\mathring{A}^{-1}$ as seen in

Fig. 2. This experimental result unambiguously indicates a substantial three-dimensionality of the FS of $1T$-VSe$_2$. Figure 2(f) shows the ARPES intensity plot at E_F as a function of k_y and k_z in the plane shown in Figs. 2 (a) and (b). Bright areas correspond to the FS. The k_z in the LM direction was estimated by using the same inner potential V$_0$ as obtained from the normal-emission measurements in Fig. 1. As clearly seen in Fig. 2(f), the FS is not straight along the k_z direction, showing a considerable wiggling at around $k_z = 2.8$ $\mathring{A}^{-1}$ and 2.95 $\mathring{A}^{-1}$. In addition, the FS appears to possess a fairly straight portion between these two k_z's. We also find other straight portions of FS around the K point at $k_z = 3.0$-3.1 $\mathring{A}^{-1}$ and around the L(H) point at $k_z = 2.5$-2.75 $\mathring{A}^{-1}$. It is expected from these experimental results that electrons on these straight portions of FS may contribute to the CDW formation by satisfying locally the nesting condition.

In order to clarify how the CDW gap evolves as a function of k_z, we show in Fig. 3(a) the ARPES spectra near E_F measured at 40 K at various positions on the FS shown in Fig. 3(b). The energy position of the peak indicated by filled circles is determined by fitting the spectra with Gaussian around the peak top. We find that the leading-edge peak in the spectra is located at 20-30 meV in the k-region near the L(H) point (spectra 1-4). Taking into account the thermal broadening effect of the Fermi-edge cutoff as well as the finite energy resolution, we conclude that the peak is actually located on E_F in this momentum region (points 1-4). Next, when one moves from point 4 to point 5, the peak position suddenly moves toward the high binding energy side and finally reaches 50 meV at points 6-8. This discernible shift in the peak position is likely caused by the suppression of spectral weight in the vicinity of E_F, namely opening of a pseudogap, due to the CDW formation. Observation of the Fermi-edge at this momentum region may be understood in terms of finite k_z-broadening effect and/or angle-integrated background. On further approaching the K point (points 10-13), the peak moves back toward E_F and is located again at 20-30 meV, indicating disappearance of the CDW-induced pseudogap. All these experimental results indicate that the momentum region of k_z = 2.8-2.95 $\mathring{A}^{-1}$, where the FS locus looks fairly flat, participates in the CDW formation with satisfying the nesting condition, while the other two straight FS portions are not essentially important for the CDW transition. This is consistent with the experimental result from the X-ray and electron-diffraction measurements,[15, 16] which reported that the nesting vector possesses a substantial component normal to the layer.[22] To the best of our knowledge, the present ARPES experiment is the first evidence for the k_z-dependent FS nesting in layered transition-metal dichalcogenide.

Next, we discuss the present observation in relation to the band calculation. Woolley and Wexler performed the layer-method band calculation[20] and found that the electronlike FS centered at the M(L) point shows considerable wiggling along the k_z direction. They have argued that this wiggling enables two different k_z portions on the Fermi surface to connect to

each other by a certain Q vector with a substantial k_z component. In this sense, the present ARPES result is consistent with the prediction from the band calculation. However, there are some notable differences between the experiment and the calculation. One is the shape of FS along the k_z direction. The present ARPES result shows that the k_F point on the LH line is closer to the ML line than that on the MK line (see Fig. 3), while the band calculation predicts the opposite behavior.[23] Another discrepancy is on the small electron pocket centered at the Γ point. The calculation has predicted that a V $3d$ band enters the occupied state below E_F around the Γ point, while there is no signature for such a band-crossing around the Γ point in the experiment as seen in Fig. 1(b). The observed discrepancy between the experiment and the calculation may be reconciled by taking into account properly the p-d hybridization strength and/or the small but finite electron-correlation among V $3d$ electrons.

Finally we comment on the number of carriers which participate in the CDW transition. It has been reported that the Hall coefficient and the intrinsic magnetic susceptibility of $1T$-VSe$_2$ show a sudden drop below T_c.[1,2] Thompson and Silbernagel discussed this reduction by using the single-carrier model and estimated that 30 % of total carriers are involved in the CDW formation. On the other hand, the present ARPES result shows that the k_z region where the pseudogap opens is a 1/4 or at most a 1/3 of the full BZ height (see Fig. 3), and it has also been found that the nesting condition is well satisfied in the portion of about 50 % of the two-dimensional FS in the $k_{x,y}$ plane.[17] By naively assuming that the total loss of the FS area due to the CDW formation is product of these two values, it is inferred that 10-20 % of carriers are removed from the FS below T_c. This value is much smaller than that estimated from the Hall coefficient and the magnetic susceptibility measurements, suggesting that the simple single-carrier picture is not realistic to understand quantitatively the CDW formation of $1T$-VSe$_2$. More sophisticated analysis which takes into account the k-dependence of the Fermi velocity as well as the hole carriers at the Γ(A) point[17] is necessary in interpreting the thermodynamic properties. Thus, it would be a challenge in future to clarify the detailed FS shape, band dispersion, and CDW gap in the entire three-dimensional BZ so as to discuss more quantitatively and to determine completely the three-dimensional nesting vector of $1T$-VSe$_2$.

4. Summary

We have performed high-resolution ARPES with synchrotron radiation on $1T$-VSe$_2$ to study the electronic structure relevant to the CDW transition. The electronlike FS centered at the M(L) point shows a remarkable wiggling with several straight portions in the k_z direction. We observed that a pseudogap opens below T_c only on a limited straight portion of the FS indicative of a substantial k_z component of the nesting vector. These experimental results indicate that the CDW transition in $1T$-VSe$_2$ is driven by the three-dimensional FS nesting despite the apparent layered crystal structure.
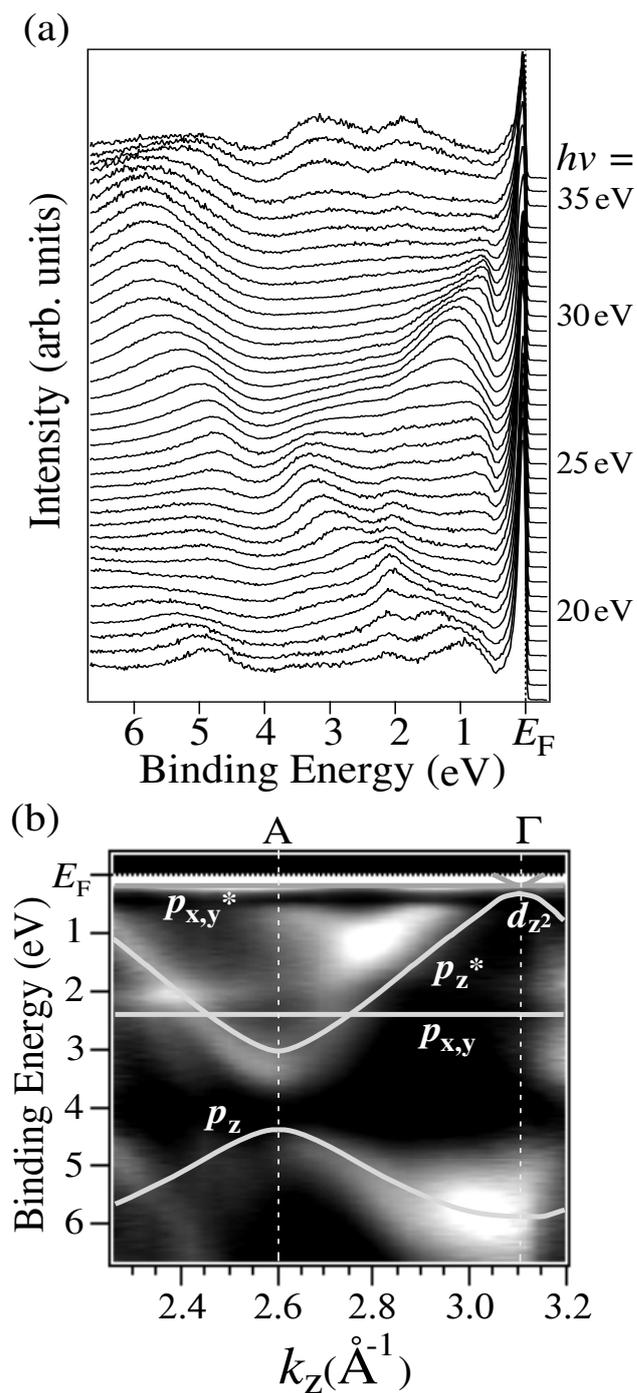
Acknowledgements

(a)

(b)

Fig. 1. (a) Normal-emission valence-band ARPES spectra of 1T-VSe$_2$ measured at 30 K. Photon energy ($h\nu$) is denoted on spectra. (b) Comparison of the experimental valence-band structure (gray scale) with the LAPW band calculation (solid lines)[11] along the ΓA direction. Bright areas correspond to bands.
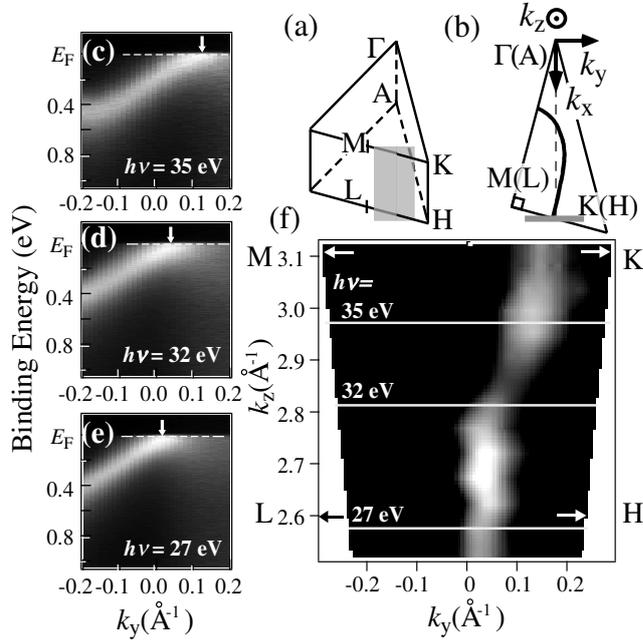
Fig. 2. (a) Schematic view of the momentum area in the BZ where the ARPES measurements were performed. (b) Two-dimensional BZ projected along the c*-axis together with the k-region of the ARPES measurements (gray line). The two-dimensional FS as a function of k_x and k_y determined by the previous ARPES experiment[17] is shown by a solid line. We define the principle k_x, k_y axes as shown by arrows. k_x is fixed at 1.12 $\mathring{A}^{-1}$ in the ARPES measurement. (c)-(e) ARPES-intensity plot (band dispersion) measured in the plane shown in Fig. 2(a) with photon energy of 35, 32, and 27 eV, respectively. Bright areas show the band. (f) ARPES-intensity plot at E_F measured at 40 K as a function of two-dimensional wave vector parallel (k_y) and perpendicular to the layer (k_z). The intensity was estimated by integrating the spectral weight within 6 meV with respect to E_F and normalized by the intensity of the area under the curve from -1 eV to 0.15 eV.
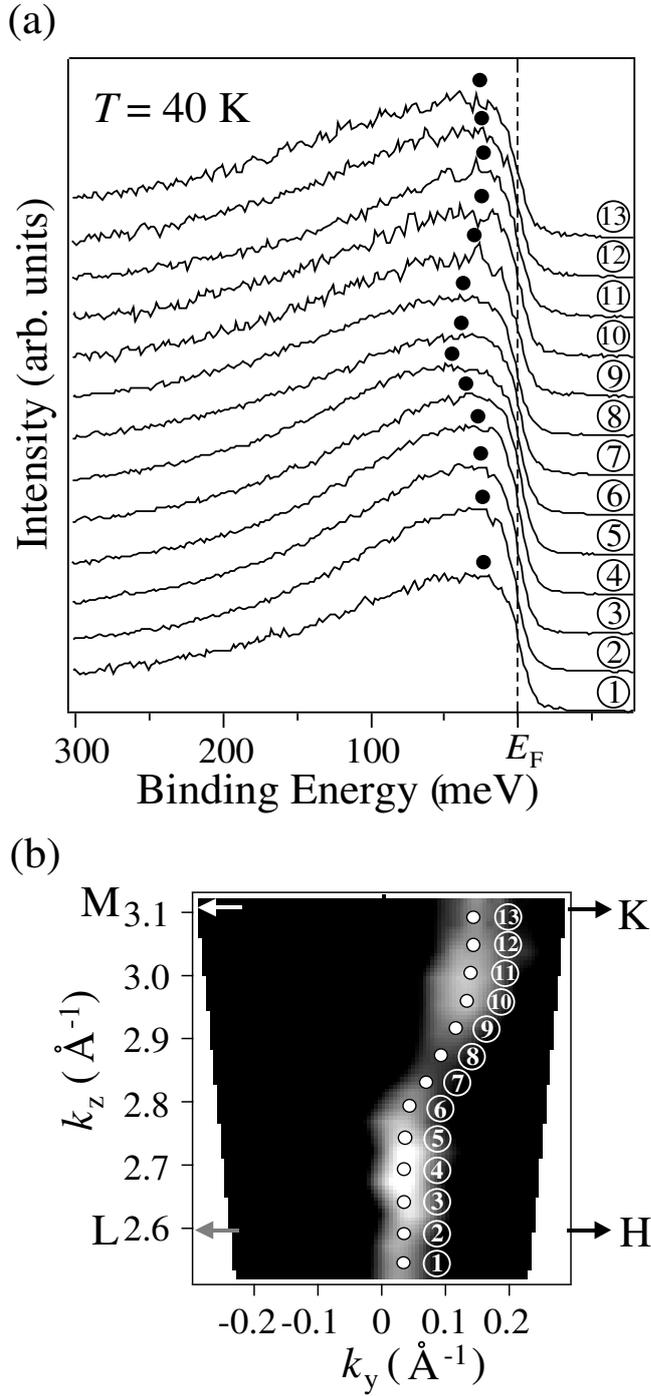
(a)

(b)

Fig. 3.   (a) ARPES spectra in the vicinity of E_F at 40 K for $1T$-VSe$_2$, measured at various positions
on the FS denoted by number (1 to 13) in (b). The peak position in spectra determined by fitting
with Gaussian around the peak top is indicated by filled circles.

References

1) A. H. Thompson and B. G. Silbernagel, Phys. Rev. B **19** (1979) 3420.

2) M. Bayard and M. Sienko, Solid State Chem. **20** (1976) 251.

3) A. Toriumi and S. Tanaka, Physica B **105** (1981) 141.

4) H. P. Hughes, C. Webb, and P. M. Williams, J. Phys. C: Solid State Phys. **13** (1980) 1125.

5) R. Claessen, I. Schafer, and M. Skibowski, J. Phys. Condens. Matt. **2** (1990) 10045.

6) A. R. Law, P. T. Andrews, and H. P. Hughes, J. Phys. Condens. Matt. **3** (1991) 813.

7) M. T. Johnson, H. I. Starnberg, and H. P. Hughes, J. Phys. C: Solid State Phys. **19** (1986) L451.

8) H. I. Starnberg, P. O. Nilsson, and H. P. Hughes, J. Phys. Condens. Matt. **4** (1992) 4075.

9) H. I. Starnberg, L. Ilver, P. O. Nilsson, and H. P. Hughes, Phys. Rev. B **47** (1993) 4715.

10) H. I. Starnberg, H. E. Brauer, L. J. Holleboom, and H. P. Hughes, Phys. Rev. Lett. **70** (1993) 3111.

11) H. E. Brauer, H. I. Starnberg, L. J. Holleboom, V. N. Strocov, and H. P. Hughes, Phys. Rev. B **58** (1998) 10031.

12) V. N. Strocov, H. I. Starnberg, P. O. Nelsson, H. E. Brauer, L. J. Holleboom, Phys. Rev. Lett. **79** (1997) 467.

13) C. Wang, C. G. Slough, and R. V. Coleman, J. Vac. Sci. Technol. B **9** (1991) 1048.

14) S. C. Bayliss and W. Y. Liang, J. Phys. C: Solid State Phys. **17** (1984) 2193.

15) K. Tsutsumi, Phys. Rev. B **26** (1982) 5756.

16) D. J. Eaglesham, R. L. Withers, and D. M. Bird, J. Phys. C: Solid State Phys. **19** (1986) 359.

17) K. Terashima, T. Sato, H. Komatsu, T. Takahashi, N. Maeda, and K. Hayashi, Phys. Rev. B **68** (2003) 155108.

18) K. Hayashi, and M. Nakahira, J. Sold State Chem. **24** (1978) 153.

19) A. Zunger and A. J. Freeman, Phys. Rev. B **19** (1979) 6001.

20) A. M. Woolley and G. Wexler, J. Phys. C: Solid State Phys. **10** (1977) 2601.

21) It is difficult to estimate quantitative value of the nesting vector normal to the layer (Q_z) from the present result, since it is necessary to cover many k_z points at different location of the electronlike FS.

22) It is noted that the first-principles band calculation by Zunger and Freeman[19] reported a similar result to the present experiment in the shape of FS along the k_z direction although they have not calculated the detailed wiggling behavior of FS.